International Journal of
INTELLIGENT SYSTEMS AND APPLICATIONS IN ENGINEERING
ISSN:2147-6799 www.ijisae.org Original Research Paper

Design of Intelligent Predictive Model for Ionospheric Disturbance in IRNSS

R. Manaswini [1, a)] and G. Raju[2, b)]

Submitted: 26/05/2023 **Revised**: 08/07/2023 **Accepted**: 27/07/2023

Abstract.: The Indian regional navigation satellite system is one of the important missions of ISRO which will mainly concentrate in providing real précised position and timing information. Ionosphere is a important layer of Earth's atmosphere that effect the electromagnetic signals that is transmitted and received between satellite and user introduces the error in position determination. The delay induced by ionosphere is iono delay higher the delay more will be total electron content and vice versa. Increased Iono delay and total electron content will indicate more error in position determination. A predictive model for IRNSS receiver is implemented which will estimate these factors. The data of different days are used to study the variation of ionosphere over Bangalore region using real time data of IRNSS. The study includes the accuracy determining parameter called DOP dilution of precision which has decreased as the number satellites increased which is the sign of higher accuracies of IRNSS.

Keywords: *NavIC; ionosphere; total electron content; vertical total electron content; code total electron content, DOP dilution of precision*

1. Introduction

A constellation of satellites called the Global Navigation Satellite System (GNSS) allows for precise positioning and real-time timing services. Many countries have contributed to the definition of the GNSS, which has local and global coverage. One of these navigation systems, the Indian Regional Navigation Satellite System (IRNSS), was launched by the Indian Space Research Organisation (ISRO). The accuracy of the position that is determined and its availability in real-time, the speed of position determination at a particular receiver location, the integrity, which refers to the system's capacity to operate effectively in unusual circumstances or in real-world settings, the system's capacity for uninterrupted operation, and the system's capability to provide services are some of the factors that are considered when evaluating a GNSS system's performance. Because the signal's refractive index changes and affects how it propagates, IRNSS satellite signals have a tendency to shift as they travel through a dynamic ionosphere. Thus, a propagation delay is recorded by the system that receives the data. The signal delay causes range and phase issues because the signal's characteristics change as it passes through the ionospheric layer. The satellite signal's overall delay depends on the frequency and electron content. The variations in the ionospheric TEC are what lead to the propagation effects, including group delay, phase delay, refraction, dispersion, Faraday rotation, scintillation, and scattering. The temporal variations can be described by the daily periodic sequence of activity, seasonal changes, variations depending on the 11-year sunspot cycle, and variations that typically occur every 27 days. Other factors that affect TEC levels include geography. As a result, ionospheric effects must be researched, identified in a dynamic real-time setting, and correction coefficients must be developed.

IRNSS (Indian Regional Navigation Satellite Systems), commonly referred to as NavIC (Navigation with Indian Constellation), is a constellation of seven satellites that are positioned in orbit in a figure-of-eight configuration. These satellites offer conventional location and timing services. L5 and S1 are designed to operate in a dual frequency mode, with L5 running at 1176.45 MHz and S1 at 2492.02 MHz, respectively. With a roughly 10m for civilian use and a 0.1m for military and encrypted users, the positional precision is meant to cover the Indian region and 1500 km at the borders. The designations of the five geosynchronous (four of which are completely operational) and three geostationary (three) IRNSS satellites are IRNSS 1A, 1B, 1C, 1D, 1E, 1F, 1G, and 1H, respectively.

The ionosphere, or charged region of the Earth's atmosphere, spans a distance of between 60 and 1000 km. There are a total of four distinct layers in the

[1]*Research scholar, Dept of ECE Jain Deemed-to-be University kanakapura road, Jakkasandra, post Bengaluru, Karnataka 562112, India. And Assistant Professor Dept of ECE, School of Engineering Technology Presidency University Itigalpura Rajanakunte Yelahanka Bangalore 560064.*
[2]*Professor, Dept of ECE Jain Deemed-to-be University kanakapura road, Jakkasandra, post-Bengaluru, Karnataka 562112, India*
a) Corresponding author: manaswikrishna20@gmail.com

ionosphere: D, E, F1, and F2. All four layers are present during the day, but at night the D layer disappears and the F1 and F2 join to form the F layer. The ionosphere is merely weakly ionised, but external influences such as solar radiation, magnetic field disturbances, and interplanetary drags will all have a significant impact on the total charge density in the ionosphere. This dynamic layer will affect electromagnetic signal transmission, reducing position accuracy. As the electron density varies on a monthly, weekly, daily, and seasonal basis in various geographic areas. The ionosphere's refractive index eventually changes, which typically results in delays and a change in the signals' direction of propagation into space. Figure 1 shows that the ionosphere's delay can result in significant range errors of up to 100m. How long signals must travel through the ionosphere to get to their destination depends on the total electron content (TEC) of the ionospheric atmosphere. The different ionosphere delays and errors increase together with the TEC value, posing a serious threat to a range of GNSS applications.

The ionospheric delay that satellite transmissions experience depends on the signal's frequency as well as the ionospheric layer's overall electron concentration. Interplanetary forces, magnetic storms, and incoming solar radiation all have an effect on the ionosphere's electron density or overall electron content. The amount of total electrons is not constant and varies with the solar cycle, the location of the sun during the day, as well as on a daily, weekly, monthly, and seasonal basis. TEC is always expressed in TEC units, where one TEC unit is equivalent to 1016 electrons/m2. A signal's delay always increases with the amount of time it spends in the ionosphere, and the direct vertical path exhibits changing TEC levels.

A precise measurement of TEC is required in order to map the ionospheric time delay of GNSS signals. The obtained ratios for GPS are L1/L2 = 1.28 and L1/L5 = 1.34, which are much lower than the ratio of the L5 and S1 signals for the IRNSS (S1/L5 = 2.19), which includes signals with the L1, L2, and L5 frequencies. The accuracy of TEC measurements is improved when S1 and L5 frequency signals are used because it is possible to estimate the TEC accurately when the frequency ratios are larger than average.

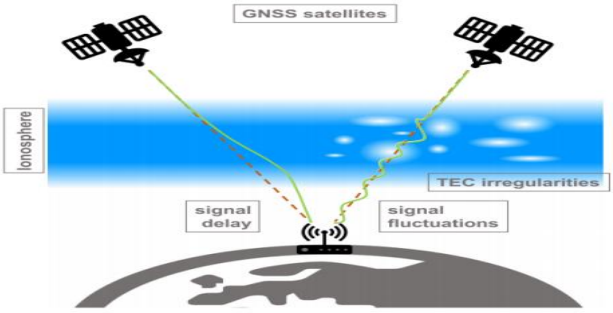

Fig 1: The ionospheric delay and fluctuations of the GNSS signal are shown. The red lines show line-of-sight GNSS satellite signals between the receiver and GNSS satellites, and the green line shows the path taken by GNSS signals due to ionosphere distortions [6].

2. Methodology

Jain University has signed an MOU with the Indian Space Research Organization's SAC (Space Applications Centre) in Ahmedabad, which has provided the receiver that can receive data from GPS and IRNSS satellites. It is designed to receive data from IRNSS signals at the L5 and S1 frequency bands as well as data from GPS signals at the L1 C/A frequency band. The equipment includes a receiver unit, an omnidirectional antenna, a low-loss RF cable, a laptop for storage and display, an Ethernet cable to link the laptop and the receiver, and a power source. The antenna is placed without any impediments on the roof to reduce multipath effects. The laptop displays and stores the data that the receiver has received in raw data format. The receiver is capable of receiving data in RINEX (Receiver Independent Exchange Format) and NMEA (National Marine Electronic Association) formats. The retrieved raw data is provided together with corresponding comma-separated value (CSV) files. These CSV files provide data about the satellite and the user's position as well as several satellite data characteristics and relevant calculations.

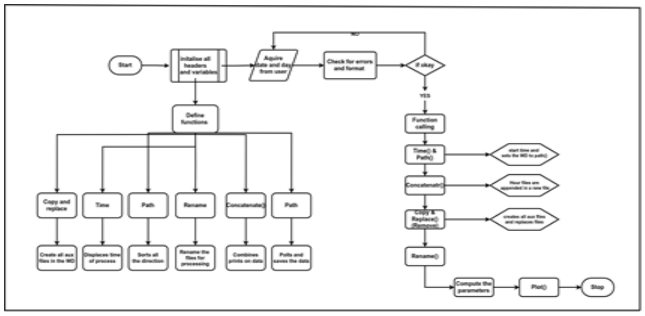

Fig 2: The above diagram indicates the methodology of the automated module.

In this paper, an automated model is developed to quickly estimate VTEC and TEC, and characteristics that are influenced by ionospheric variations are explored. Various techniques can be utilised to derive the TEC content of a certain area. For the measured values of TEC in the region of interest, the ionosphere's delay is calculated using both L5 and S1 frequency signals. All available satellite data is considered for a comprehensive analysis, and the appropriate TEC values are calculated. Dual frequency receivers like IRNSS receivers, which provide both L5 and S1 frequency, can use a method called code TEC measurement to ascertain the total electron content. The pseudo-range values set by both frequencies at a certain time are taken into account when calculating the overall electron content. Pseudo-range is used to estimate the satellite's distance from the user because the exact position of the satellite cannot be known. Four satellite signals must be gathered in order to estimate a position accurately. By dividing the time, it takes for signals to travel from a satellite to a receiver by the speed of light, the pseudo ranges can be computed.

The pseudo-range's value is determined by the

$$P_{R1}=\rho + c\,(\Delta t_r - \Delta t_s) + I_1 + T + b^P_{1r} + b^P_{1s} + m^P_1 + \varepsilon^P_1 \quad (1)$$

$$P_{R2}=\rho + c\,(\Delta t_r - \Delta t_s) + I_2 + T + b^P_{2r} + b^P_{2s} + m^P_2 + \varepsilon^P_2 \quad (2)$$

The PR1 and PR2 in the equation above denote, respectively, the pseudo-range in metres of the S1 frequency (2492.028 MHz) and the L5 frequency (1176.45 MHz). T represents tropospheric delay in metres, b is instrumental biases of both the receiver and the satellite, tr and ts indicate, and m1 and m2 are multipath in metres. I1 and I2 are ionosphere time delay in metres of S1 and L5, respectively. In metres, stands for the geometric range, and 1 and 2 for the thermal noise. Eliminate the multipath and thermal noise from the aforementioned calculations by subtracting 1 from 2 and taking into account

$$P_{R1}-P_{R2}=I_1-I_2+(b^{P1}_r+b^{P1}_s) \quad (3)$$

Where $b^P{}_r = b\ b^P{}_r = b^P{}_r$

Ionospheric delay, which is represented by the delay caused by the ionospheric layer, is provided by the following equation.

$$I_f=\left(\frac{40.3}{f^2}\right)TEC \quad \text{[in meters]} \quad (4)$$

$$CTEC=\frac{1}{40.3}\left[\frac{f_1^2 f_2^2}{f_1^2 - f_2^2}\right]+\left[P_{R2}-P_{R1}-(b^{P1}_r+b^{P1}_s)\right] \quad (5)$$

$$CTEC=4.4912[P_{R2}-P_{R1}] \quad (6)$$

$$VTEC=CTEC\times\cos\left\{\arcsin\left(R_e\times\frac{\cos\theta}{R_e+h_{max}}\right)\right\} \quad (7)$$

Where the value of Re (Radius of Earth) = 6378 km, h_{max}=350 km, θ = elevation angle in a given ground station.

The ionospheric layer, which is 300–400 km high, influences a satellite's line of sight to a user. The ionospheric piercing point is at the junction altitude. The average ionospheric pierce point for navigational purposes on the Indian subcontinent is 350 km. The many other satellite metrics frequently vary as a result of ionospheric changes, which affects and modifies the performance as a whole. The automated model additionally considers a number of parameters, such as elevation angle, pseudo-range, signal-to-noise ratio, GDOP, and Doppler. The elevation angle, which is an important consideration in identifying ionospheric disturbances, is the vertical angle formed by the satellite and the horizontal of the Earth's horizon with respect to the location of the antenna on the planet in the direction of travel. The dual-frequency automated module is efficient and flexible enough to be interfaced with any kind of computer system. It was created for the purpose of measuring and identifying ionospheric influence on IRNSS satellites. The module is designed to use one day's worth of complete data and is based on the time of week count values (TOWC) for both the L and S band. Depending on the processing speed of the system, the detecting module runs in around 2 minutes for a standard computer with a workstation.

The ionosphere is an inhomogeneous and anisotropic substance. With time, the density of electrons in a certain area change. Total electron concentration is measured using the IRNSS L and S bands. Each of the seven satellites' L- and S-band displays are produced by the design. Since they are adversely affected by significant ionosphere disturbance, signal-to-noise ratio, doppler, DOP, pseudo-range, elevation, and other position-related variables are taken into consideration. The module is designed to evaluate two forms of ionospheric total electron content: code total electron content (CTEC) and vertical total electron content (VTEC).

The user must explicitly provide the date in dd-mm-yyyy format for which the impacts of ionospheric analysis need to be assessed. Basically, the automatic module In simple terms, the automatic module completes six major tasks. The system determines if the requested data is contained in the IRNSS database based on user requests. The user-specified file is set as the working directory,

and this information is then converted into file names because logs are given names based on dates. The user input is initialised and organised in the following code. The working directory information will be stored in the variable in a different fashion; this is useful since it will be compared to the input in a later phase. In order to separate particular data, a variable is iterated from 0 to 1 for the day, 3 to 4 for the month, and 6 to 10 for the year.

The accuracy levels of any navigation system are measured in terms of dilution of precision, always for accuracy levels to be higher the geometric relationship between measuring device and satellite should be good. The system with less value of DOP will always have higher accuracy levels. The Vertical Dilution Precision (VDOP) Geometric Dilution Precision (GDOP), Position Dilution Precision (PDOP), Horizontal Dilution Precision (HDOP), Time Dilution Precision (TDOP) and are other parameters of DOP.

The geometric strength of the operational satellite configuration is exhibited by the DOP value. The value of DOP is higher when all visible satellites are closers and lesser is the accuracy and less the DOP value higher is accuracy. DOP also indicated the current geometric properties of the available satellites.

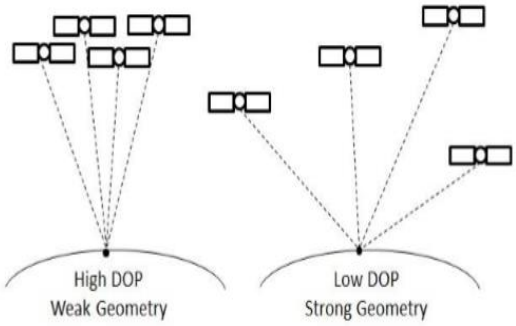

Fig 3: In the above pictorial representation it is observed that the position of the satellites must be distributed and oriented properly so that stronger geometry can be achieved with higher accuracy.

Positional accuracy can be represented in the form of equation as

Accuracy = DOP x User equivalent distance error

Accuracy in the above equation is given by ratio of positioning error to mean positioning accuracy.

DOP Value	Rating	Inference
1	Ideal	This level of DOP is suitable for applications demanding highest precision levels.
1-2	Excellent	This level of DOP will facilitate position measurements to considerable accurate levels.
2-5	Good	In this range the system performance can be considered as minimum suitable in concluding the accurate decision.
5-10	Moderate	The measured value in this particular range can be but the quality can be improved.
10-20	Fair	This level clearly indicates low confidence level, measured position values can be considered for rough estimations for particular locations.
>20	Poor	The measure values are completely inaccurate up to 300m hence the measurements can be discarded.

Table1: The above value indicates the inference that can be drawn from DOP values.

PDOP or GDOP indicated the error caused by the relative position of the GNSS satellites. It is observed that the more signals receiver can receive from different satellites in the constellation, precision value increases. The wider angular distribution and separation in between the satellites in the constellation higher accuracy can be achieved.

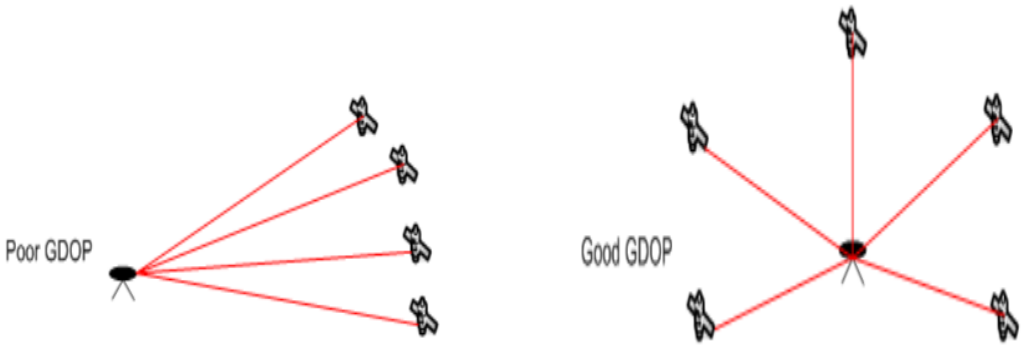

Fig 4: The above diagram indicated how the distribution of satellites will result in good GDOP.

Concept in determining position using IRNSS

The trilateration is the method used to determine any location or position point on the earth using any satellite system. The trilateration is a sublunary surveying technique. Using IRNSS receiver the range or distance between satellite and earth can be determined. For any given user point the 3D positions such as latitude, longitude and altitude can be mapped for different satellites. The intersection point of recoded ranges of minimum three satellite gives the location identity and one more additional rage data of satellite is required in order to resolve timing offset problems.

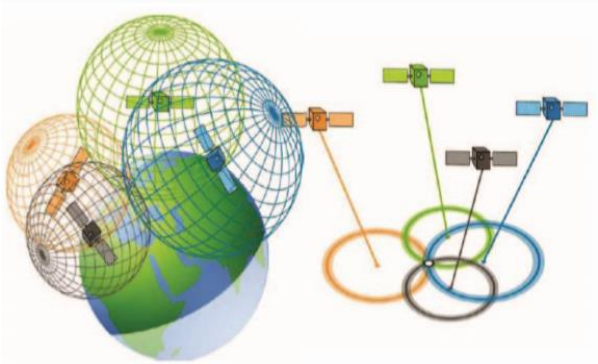

Fig 5: Position determination representation**.**

The navigation receiver unit computes the three-dimensional coordinates, by simultaneous measurement of pseudorange from four or more satellites. The measurements are biased range between the antenna of each satellite and the receiver antenna. The cross correlation of the pseudorange noise code sent from each satellite yields the pseudorange values. The pseudorange accuracy that is measured and fidelity of the processing model for determination, provides the complete accuracy.

The below equation is used to compute pseudorange

$$P = \rho + c\,(dT - dt) + d_{ion} + d_{trop} + e \quad \ldots\ldots\ldots 1$$

P indicates Pseudorange, geometric range between antenna and the satellite during the time of reception of signal is indicated by ρ, dt, dT indicates satellite clock offset and receiver clock offset respectively, d_{ion} is ionospheric delay, d_{tro} is tropospheric delay introduce to the signal that passes through ionosphere and troposphere during its transmission, c stands for speed of light at vacuum, e stands for noise measurement and multipath an unmodeled effect.

3. Results and Discussion

The investigations and research conclusions use the data from the receiver located at Jain University in Bangalore. The dates are selected based on their availability in the database, and after additional research and processing, a few instances of dates that are taken into consideration and which have a greater impact on the ionosphere during high solar flare conditions are shown. The ionospheric influence detection module generates about 120 charts, including plots of combined values of multiple satellite parameter values. The identification of the ionospheric disturbance is supported by a few key findings that are presented. The estimated values of multiple satellites are included in consolidated graphs, and independent satellite value plots are also available for alternative studies if necessary. The total number of ionospheric disturbances that are seen over a specific time period is influenced by the overall electron concentration. When TEC, either VTEC or CTEC, increases, ionospheric disturbances increase as well.

TDOP) are acronyms for these variables.

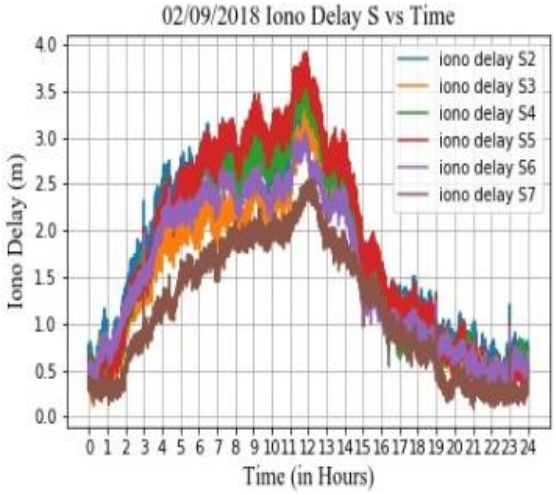

Fig 6: Graph showing the anticipated iono delay for the S band for the IRNSS satellites. For the date of 2/09/2018, S5, which is satellite 1E, recorded the greatest value, which ranges from 3 to 5 metres, while S7, which is satellite 1G, recorded the lowest value, which is approximately 2.5 metres.

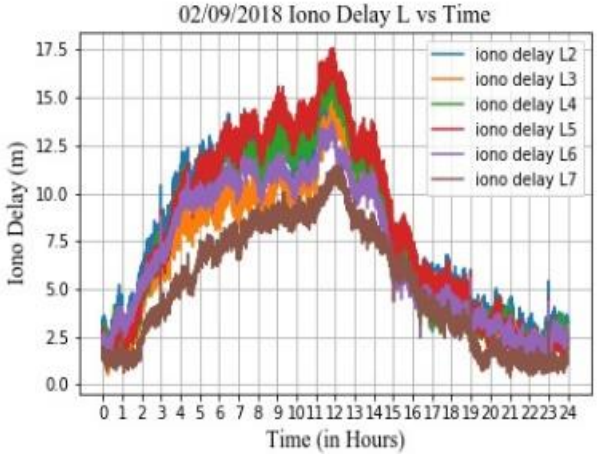

Fig 7: Graph showing the anticipated iono delay for the L band for the IRNSS satellites. For the date of 2/09/2018, L5—satellite 1E—recorded the highest value, which is roughly 17.5m, while L7—satellite 1G—recorded the lowest value, which is roughly 11m (in metres).

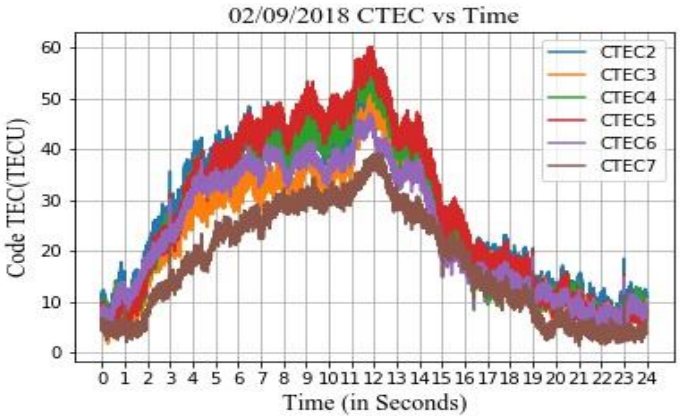

Fig 8: Graph showing the IRNSS satellites' estimated CTEC. For the date of 2/09/2018, CTEC5 (satellite 1E) recorded the greatest value, which is roughly 60TECU, while S7 (satellite 1G) recorded the lowest value, which is roughly 40TECU.

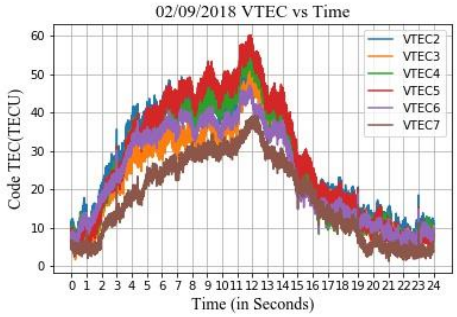

Fig 9: Graph showing the estimated VTEC for the L band on the IRNSS satellites. For the day of 2/09/2018, L7, which is satellite 1G, recorded the greatest value, which ranges from 55 to 80 TECU, while S5, which is satellite 1E, recorded the lowest value, which ranges from 10 to 40 TECU.

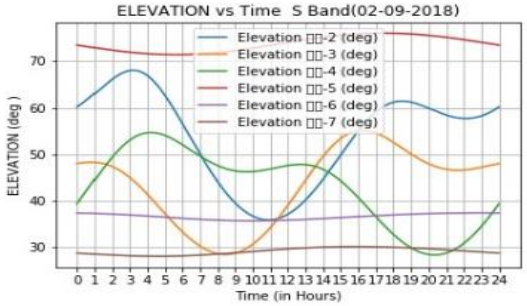

Fig 10: Graph showing the IRNSS satellites' elevation angles in the L band. The maximum value, which is over 70 degrees, was obtained by S5 (satellite 1E). For the day of 2/09/2018, S7 (satellite 1G) recorded the lowest temperature below 30 degrees.Higher levels of TEC are reported because the satellite that recorded the highest elevation angle was subjected to more ionosphere disturbance.

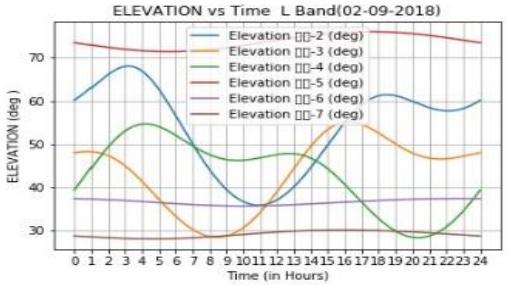

Fig 11: Graph showing the IRNSS satellites' elevation angles in the L band. The maximum figure, which is above 70 degrees, was obtained by L5, which is satellite 1E. For the date of 2/09/2018, L7, one of the 1G satellites, recorded the lowest temperature below 30 degrees.Higher TEC values are reported because the satellite that recorded the highest elevation angle was exposed to a stronger ionosphere.

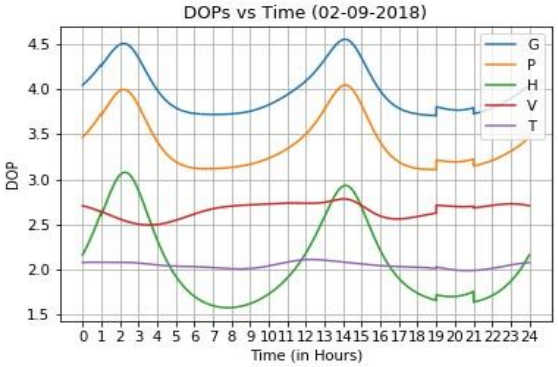

Fig 12 Graph indicating the DOP estimated for the IRNSS satellites for the date 2/09/2018. G,P,H,V,T are respectively Geometric(GDOP), Position (PDOP), Horizontal(HDOP), Vertical (VDOP) and Time Dilution Precision (TDOP).

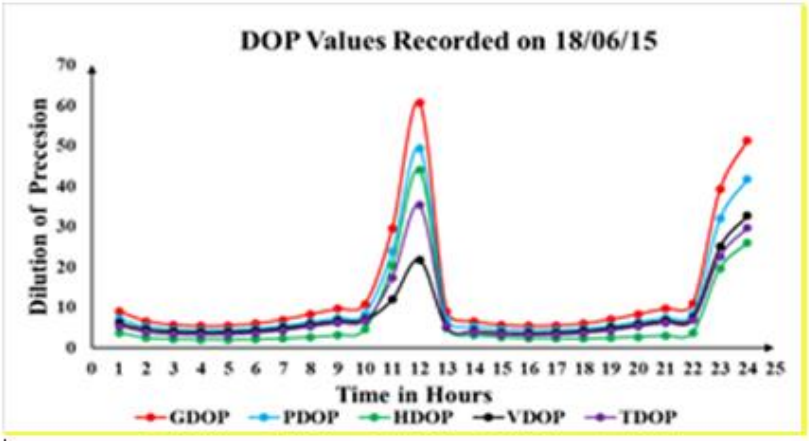

Fig 13: The above graph indicates the value of DOP's mapped on 18/06/2015, it is observed that the range of all DOP's are between 0 to 10. This value is measured during the year 2015 which indicates the measurement of position accuracy is moderate. The highest peak recorded 65 value which coincides with the occurrence of solar flare. (16:30 to 18:25).

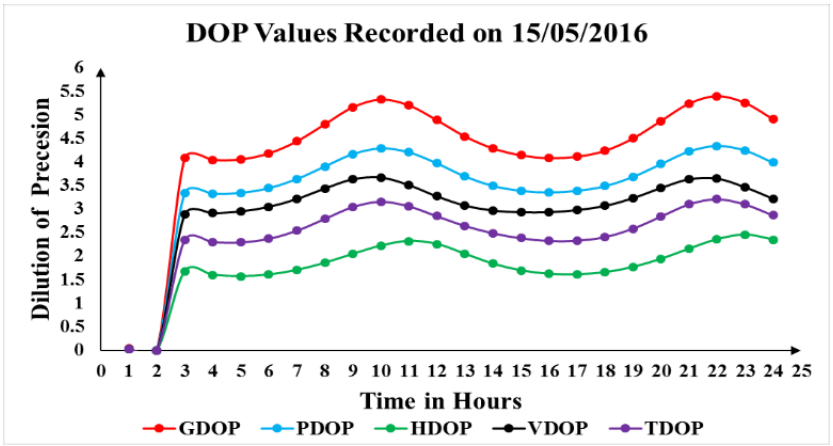

Fig 14: The above graph indicates the value of DOP's mapped on 15/05/2016, it is observed that the range of all DOP's are between 0 to 6. This value is measured during the year 2016 which indicates the measurement of position accuracy is moderate. The initially reading is recorded to be 0 because of the occurrence of solar flare on the previous day.

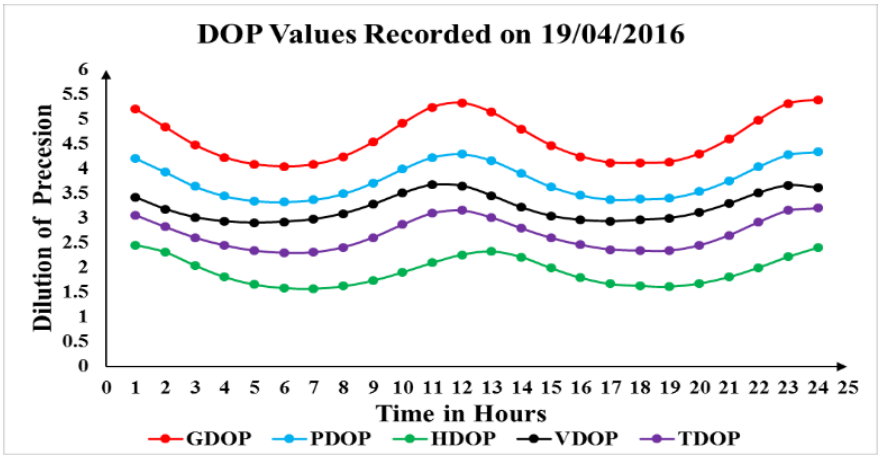

Fig 15: The above graph indicates the value of DOP's mapped on 19/04/2016, it is observed that the range of all DOP's are between 2.5 to 5.5. This value is measured during the year 2016 which indicates the measurement of position accuracy is good. The decreasing trend in the DOP's is observed which indicates the improving accuracy in position measurement.

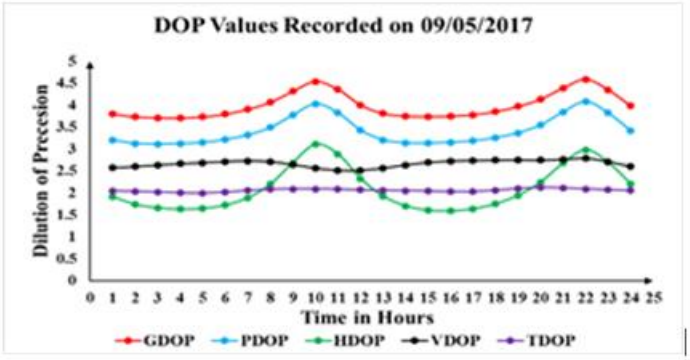

Fig 16: The above graph indicates the value of DOP's mapped on 9/05/2017, it is observed that the range of all DOP's are between 1.5 to 4.5. This value is measured during the year 2017 which indicates the measurement of position accuracy is good.

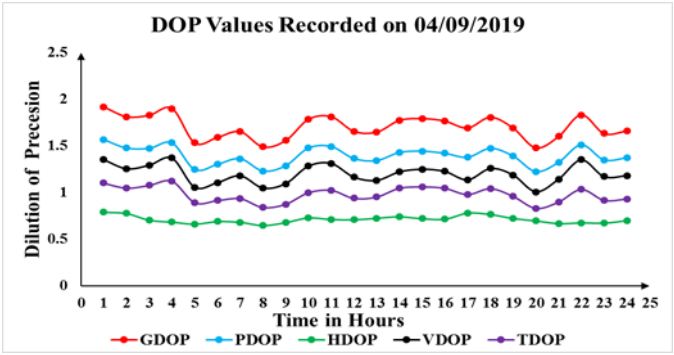

Fig 17: The above graph indicates the value of DOP's mapped on 4/09/2019, it is observed that the range of all DOP's are between 0.5 to 2. This value is measured during the year 2019 which indicates the measurement of position accuracy is moderate. The decreasing trend in the DOP's is observed which indicates the improving accuracy in position measurement.

Lower frequencies are more vulnerable to ionospheric perturbations than higher frequencies. The overall electron content recorded in the VTEC, CTEC, and iono delays in the L5 band is greater compared to the S-band. The dilution of precision values, which establish precision levels, should always be between 1 and 2 units for the system to function at its best. However, numerous changes are observed during ionospheric variations, and the value has even reached 6, which is unacceptable. The dynamic ionospheric layer for both VTEC and CTEC is in the range of 1 to 25 metres on different dates, and the total electron content values are in the range of 10 to 80 TECU. It has affected specific dates and satellite operation. Higher values of iono delays typically cause a greater mismatch in range determination. demonstrates how long-lasting ionospheric turbulence is. Additionally, it is found that the delay suffered by S-band frequency significantly smaller within 5m compared to L band 25m, leading one to conclude that ionosphere effects are most noticeable at lower frequencies and less so at higher frequencies. Iono delay demonstrated the delay. The concept of DOP is essential in position determination. In the year 2019 DOP value recoded is 2 which indicates the excellent performance of IRNSS satellites in position determination. The constellation is planned to be extended to eleven satellites which may even improve the coverage and accuracy of the system. It is also expected that in near future the IRNSS chips will be included in the smart phones that will be advantageous to civilian applications. In this paper it is clearly examined the change in the DOP values in the reginal navigation system.

4. Conclusion

The model that was developed can be used to identify ionospheric disturbances in IRNSS data for both the L and S frequency bands. It is essential to identify and eliminate these disturbances since the ionosphere has a direct impact on the system's performance accuracy. To find correction factors, the module is a great tool. The model may be effectively applied to any IRNSS receiver interface system; on a system with 4GB RAM, ionospheric disturbances can be located and output graphs can be generated in less than two minutes. Additionally, time can be cut even more in half with more powerful computing devices. When deciding on a position, the DOP concept is crucial. The DOP value recoded for the year 2019 is 2, which demonstrates the superior performance of IRNSS satellites in determining position. Eleven satellites are planned for the constellation, which could further improve system accuracy and coverage. Additionally, it is anticipated that IRNSS chips, which are useful for civilian applications, would soon be found in smartphones. The

shift in the DOP values in the conventional navigation system is thoroughly explored in this research.

5. Acknowledgments

The data for the study's research endeavor came from the IGS receiver device that the ISRO Space Application Centre Ahmedabad (SAC) put at Jain University Bangalore. The ability to finish the space weather-related and IRNSS performance-related experiments was made possible thanks in large part to ISRO SAC Ahmedabad, for which the authors are grateful.

References

[1] Aa, E., Zou, S., Eastes, R., Karan, D. K., Zhang, S.-R., Erickson, P. J., & Coster, A. J. (2020). Coordinated ground-based and space-based observations of equatorial plasma bubbles. *Journal of Geophysical Research: Space Physics*, **125**(1), e27569. https://doi.org/10.1029/2019JA027569

[2] Aa, E., Zou, S., & Liu, S. (2020). Statistical analysis of equatorial plasma irregularities retrieved from Swarm 2013–2019 observations. *Journal of Geophysical Research: Space Physics*, **125**(4), e27022. https://doi.org/10.1029/2019JA027022

[3] Aa, E., Zou, S., Eastes, R., Karan, D. K., Zhang, S.-R., Erickson, P. J., & Coster, A. J. (2020). Coordinated ground-based and space-based observations of equatorial plasma bubbles. *Journal of Geophysical Research: Space Physics*, **125**(1), e27569. https://doi.org/10.1029/2019JA027569

[4] ground-based and space-based observations of equatorial plasma bubbles. *Journal of Geophysical Research: Space Physics*, **125**(1), e27569. https://doi.org/10.1029/2019JA027569

[5] Aa, E., Zhang, S.-R., Erickson, P. J., Coster, A. J., Goncharenko, L. P., Varney, R. H., & Eastes, R. (2021). Salient Midlatitude Ionosphere-Thermosphere Disturbances Associated With SAPS During a Minor but Geo-Effective Storm at Deep Solar Minimum. *Journal of Geophysical Research: Space Physics*, **126**(7), e29509. https://doi.org/10.1029/2021JA029509

[6] *Signal-in-Space ICD for INCOIS Messages via NaVIC Messaging Service* 1st ed., Indian Space Research Organization., ISRO, India, 2019, pp. 1-134.

[7] Aa, E., Zhang, S.-R., Erickson, P. J., Coster, A. J., Goncharenko, L. P., Varney, R. H., & Eastes, R. (2021). Salient Midlatitude Ionosphere-Thermosphere Disturbances Associated With SAPS During a Minor but Geo-Effective Storm at Deep Solar Minimum. *Journal of Geophysical Research: Space Physics*, **126**(7), e29509. https://doi.org/10.1029/2021JA029509

[8] Real-time (Quicklook) Dst index, World Data Center for Geomagnetism, Kyoto. https://wdc.kugi.kyotou.ac.jp/dst_realtime/index.html. Accessed on 20th April 2022.

[9] Space Weather Prediction Center, National Oceanic and Atmospheric Administration. https://www.swpc.noaa.gov/phenomena/f107-cm-radio emissions. Accessed on 15th April, 2022.

[10] Aa, E., Zhang, S.-R., Wang, W., Erickson, P. J., Qian, L., Eastes, R., et al. (2022). Pronounced Suppression and X-Pattern Merging of Equatorial Ionization Anomalies After the 2022 Tonga Volcano Eruption. *Journal of Geophysical Research: Space Physics*, **127**(6), e2022JA030527. https://doi.org/10.1029/2022JA030527

[11] Aa, E., Zou, S., Eastes, R., Karan, D. K., Zhang, S.-R., Erickson, P. J., & Coster, A. J. (2020). Coordinated

[12] Desai MV, Shah SN (2020) An observational review on influence of intense geomagnetic storm on positional accuracy of NavIC/IRNSS system. IETE Tech Rev 37(3):281–295. https://doi.org/10.1080/02564602.2019.1599739

[13] Ratnam, D. V., T. R. Vishnu, and P. B. S. Harsha, "Ionospheric gradients estimation and analysis of S-band navigation signals for NAVIC system," *IEEE Access*, Vol. 6, 2018 pp66954–66962.

[14] M. Ravi Kumar, M. Sridhar, D. Venkata Ratnam, P. Babu Sree Harsha, S. Navya Sri, "Estimation of ionospheric gradients and vertical total electron content using dual-frequency NAVIC measurements," *Astrophys Space Science*, 2019 pp. 1-9. https://doi.org/10.1007/s10509-019-3535-y

[15] Abe, O. E., X. Otero Villamide, C. Paparini, S. M. Radicella, and B. Nava, "Analysis of a grid ionospheric vertical delay and its bounding errors over West African sub-Saharan region," J. Atmos. Solar-Terrestrial Phys., Vol. 154, 67–74, Feb. 2017, doi: 10.1016/j.jastp.2016.12.015.

[16] Jiang, H., Z. Wang, J. An, J. Liu, N. Wang, and H. Li, "Influence of spatial gradients on ionospheric mapping using thin layer models," *GPS Solut*., Vol. 22, No. 1, Jan. 2018, doi: 10.1007/s10291-017- 0671-0.

[17] T. Biswas, P. Banerjee, "*Testing the conformity of GPS and IRNSS in terms of ionospheric delay and position errors,*" 5th International Conference on Signal Processing and Integrated Networks, 2018, pp. 159-163.

[18] M. Ravi Kumar, M. Sridhar, D. Venkata Ratnam, P. Babu Sree Harsha, S. Navya Sri, "Estimation of ionospheric gradients and vertical total electron content using dual-frequency NAVIC measurements," *Astrophys Space Science*, 2019 pp. 1-9.

[19] Abe, O. E., X. Otero Villamide, C. Paparini, S. M. Radicella, and B. Nava, "Analysis of a grid ionospheric vertical delay and its bounding errors over West African sub-Saharan region," J. Atmos. Solar-Terrestrial Phys., Vol. 154, 2017, pp67–74

[20] Interface control document (icd) of distress alert transmitter - second generation (dat-sg) 2nd ed., Indian Space Research Organization., ISRO, India, 2019, pp. 1-30.

[21] K.Ramulamma, K.C.T.Swamy "*Estimation and Analysis of IRNSS Satellites Differential Code Biases using Real Data,"* International Journal of Recent Technology and Engineering Vol-8 Issue-3, 2019, pp.740-743

[22] Shivani Sinha, Ritika Mathur, Sharat Chand Bharadwaj, Anurag Vidyarthi, B S Jassal, A K Shukla, "*Estimation and Smoothing of TEC from NavIC Dual Frequency Data*," 4th International Conference on Computing Communication and Automation, 2018, pp. 1-5.

[23] D. Venkata Ratnam, J. R. K. Kumar Dabbakuti, N. V. V. N. J. Sri Lakshmi "Improvement of Indian-Regional Klobuchar Ionospheric Model Parameters for Single-Frequency GNSS Users*," IEEE Geoscience and Remote Sensing Letters*, Vol. 15, pp.971-975, 2018.

[24] Sruthi Samyuktha Sathyana, Thangadurai N, Saribala Priyanka, Gutti VaddiNavya, Gayathri K M, "Study of Azimuth Angle and Elevation Angle Variations of IRNSS/NavIC Signals" *Universal Journal of Electrical and Electronic Engineering* vol.6(5), pp. 373-382, 2019, DOI: 10.13189/ujeee.2019.060508.

[25] Q.J. Mohd, D.S. Achanta, V.K.R. Nalam., T.K. Pant., "Comparison of TEC estimation techniques using S1 and L5 signals of IRNSS," *Radioelectronics and Communications Systems*, Vol 61 No. 7, pp. 306-316, July 2018. doi: https://doi.org/10.3103/S0735272718070038

[26] Ratnam, D. V., T. R. Vishnu, and P. B. S. Harsha, "Ionospheric gradients estimation and analysis of S-band navigation signals for NAVIC system," *IEEE Access*, Vol. 6, 66954–66962, 2018, doi: 10.1109/ACCESS.2018.2876795

[27] Dhabliya, M. D. . (2021). Cloud Computing Security Optimization via Algorithm Implementation. International Journal of New Practices in Management and Engineering, 10(01), 22–24. https://doi.org/10.17762/ijnpme.v10i01.99

[28] Anand, R., Khan, B., Nassa, V. K., Pandey, D., Dhabliya, D., Pandey, B. K., & Dadheech, P. (2023). Hybrid convolutional neural network (CNN) for kennedy space center hyperspectral image. Aerospace Systems, 6(1), 71-78. doi:10.1007/s42401-022-00168-4